Journal of Population Therapeutics & Clinical Pharmacology

RESEARCH ARTICLE

DOI: 10.53555/jptcp.v29i01.3851

SYNTHESIS, CHARACTERIZATION AND PHARMACOLOGICAL STUDIES OF METAL(II) COMPLEXES WITH HIGHLY CONJUGATIVE HETEROCYCLIC LIGANDS

B. Bincy, Joseph[1*], E.H. Edinsha Gladis[2]

[1*, 2]Dept. of Chemistry, Noorul Islam Centre for Higher Education, Kumaracoil-629180, Tamilnadu
E mail: joseph@niuniv.com; Mob: 91-8610748179*

***Corresponding Author:** B. Bincy, Joseph
*Dept. of Chemistry, Noorul Islam Centre for Higher Education, Kumaracoil-629180, Tamilnadu
E mail: joseph@niuniv.com; Mob: 91-8610748179*

Abstract
A novel bioactive metal(II) complexes with the molecular formulae of [$M^{II}L$] (where M= Cu(II), Ni(II), Co(II) and Zn(II); L = heterocyclic ligand, curcumin derivative) were synthesized. They were characterized using elemental, thermal analysis, molar conductance, cyclic voltammetry, magnetic moment measurements as well spectral (FT-IR, UV–Vis and ESR) techniques. Powder X-ray diffraction spectral data has been utilized for the study of crystalline properties of metal complexes. The DNA interaction study performed by UV–visible spectroscopy as well as by molecular docking suggests the tested compounds interact with DNA through intercalation mode. The oral glucose tolerance test was used for the hypoglycemic test, and the phenobarbitone-induced sleeping duration test was used to evaluate the CNS depressant activity of metal Schiff base complexes.

Keywords: Complexes; catalytic; copper enzymes; intercalation; mimetic.

1. Introduction

The world is getting worse because there are more and more everyday activities that pose a severe threat to humanity. Antibiotic resistance is perhaps the greatest hazard of the twenty-first century and might be a "potential tragedy" for both human wellbeing and the world economy, according to the World Economic Forum and the World Health Organisation. Antibiotic resistance is worryingly increasing, which makes the creation of novel classes of antibacterial candidates necessary. Antimicrobial chemotherapy was made possible with the development of several antibiotic medications, including Daptomycin, GAR936 Linezolid, and Oitavancin. Metallo-drugs are one of the treatment strategies being considered. Since metal complexes interact with intracellular biomolecules, limit enzymatic activity, enhance lipophilicity, alter the function of the plasma membrane, and disrupt the cell cycle, they are being investigated as possible candidates.

The clinical success of platinum-based anticancer drugs such as cisplatin, carboplatin and oxaliplatin [1,2] has stimulated the exploration of new metallodrugs with distinct structural and mechanistic profiles, which may be able to reduce side effects like nausea and kidney toxicity,[3] widen the spectrum of sensitive tumors, and overcome platinum resistance. Among these metallodrugs, organometallic compounds, which are suitable for rational drug design due to their

versatile structures, can bridge the gap between classical inorganic and organic anticancer drugs and show improved efficacy and tolerability.

Metal–organic frameworks are gaining intensive attention due to their wide practical utility as dyes, extractants, drugs, pesticides, catalysts, magnetism, host–guest chemistry [1–5]. Usually, multidentate organic ligands containing coordination sites of N and/or O donors play key roles in construction of novel metal–organic frameworks [6].

Due to its bioavailability, copper has a rich and varied history in medicinal chemistry, in the form of compounds used as antibacterial and anticancer agents [4-6]. There is considerable interest in using copper in place of platinum in therapeutic agents, because it is much better tolerated, mainly as a result of natural biological pathways which regulate Cu levels [4]. In nature, Copper is a fundamental metal for living systems having unique chemical properties that allow it to plays divers roles in cellular functions chemistry [8]. Its biological significance is ascribed to the capability of copper to catalyze oxidation reduction (redox) chemistry [8]. The copper containing enzymes and proteins played a significant role in biocatalytic process with different mechanism of action [9]. Inspired and motivated from metalloenzymes and proteins, researchers have performed different catalytic reactions in the presence of transition metal complexes as catalyst such as oxidation, epoxidation, carboxylation, hydrogenation and other functional group transformations [10-15]. Copper(II) ion plays an important role in biological systems, supramolecular chemistry [7–11] and various enzymatic reactions, such as catechol oxidase [12–22] and catalase like activity. Catechol oxidase has been successfully conducted by Krebs and co-authors since 1998 [23]. Catechol oxidase, in other words the polyphenol oxidases, oxidizes phenolic compounds in the presence of dioxygen to the corresponding quinone [24].

Zinc(II) is one of the most abundant essential ions in the human body. It is found in all body tissues [1], Zinc-containing enzymes are considered an attractive target for drug therapy and their inhibitors are included in the armamentarium of modern medicine against human diseases such as cardiovascular, neurological, infectious and metabolic diseases as well as cancer [13].

To develop functional models similar metal binding sites to metalloenzymes or metalloproteins that allows the desired chemical transformation and enhanced catalytic properties [29-31]. Metal ions are important part of many natural proteins, providing structural, catalytic and electron transfer functions. Copper oxidases with environmentally friendly oxidants, O_2 have performed selective organic transformations. Motivated and develop copper complexes which mimics metalloenzymes have shown higher reactivity in the oxidation of alcohols under aerobic conditions.

In this regard ternary copper(II) complexes containing amino acid and nitrogen base afford donor sites which match the native copper proteins. Among the studied nitrogen bases, 1,10-curcumin has been the most attractive due to its various functions [24]. Furthermore, the ternary copper(II) complexes can serve as oxidase models that provide a better understanding of the catalytic pathway of the native copper-enzyme [32].

Metal complexes of Schiff-base ligands play an important role in material science and chemical research, due to their interesting properties and diverse structural aspects [33, 34]. The structural variability of transition metal complexes of multidentate Schiff-base ligands with desired molecular geometry and the structure–function correlation of the resulting complexes has been the subject of intensive research recently [35]. Moreover, several studies [36] showed that due to the presence of a lone pair of electrons in nitrogen atom of the azomethine group, HC=N is of biological importance and attracts the interest of biological inorganic chemists.

In the present investigations was focused on the synthesis of Schiff-base ligand through condensation of curcumin derivative. We also prepared the synthesis of new complexes of Co(II), Zn(II), Ni(II) and Cu(II) derived from this hexadentate Schiff-base ligand (Scheme 1). The complexes and ligand have been investigated by FT-IR, Visible spectra (UV–Vis) and proton nuclear magnetic resonance (^{1}H NMR) and cyclic voltammetry (CV). The antibacterial activity against some selected bacterial strains and antioxidant properties of these metal complexes are also reported and discussed. The oral glucose tolerance test was used for the hypoglycemic test, and the

phenobarbitone-induced sleeping duration test was used to evaluate the CNS depressant activity of metal Schiff base complexes.

2. Experimental

All the solvents and chemicals used in the synthesis were purchased from commercial suppliers and purified when necessary. The completion of the reaction was monitored by thin layer chromatography performed on Merck precoated silica gel plates. Silica gel (60–120 mesh size, Merck) was used for column chromatography for purification purpose.

Carbon, hydrogen and nitrogen were estimated by using Elemental Analyzer Carlo Erba EA1108 analyzer. The IR spectrum of synthesized compounds was recorded on a Shimadzu FTIR Affinity-1 Spectrophotometer in the 4000-400 cm^{-1} region in KBr disc. The electronic spectra of the complexes were recorded in spectral grade DMSO on a Systronics UV-Visible spectrophotometer in the region of 200-1100 nm. The ^{1}H-NMR spectrum of the ligand was recorded in DMSO-d_6 on a BRUKER 400 MHz spectrometer at room temperature using TMS as an internal reference. Proton coupling patterns are described as single (s), double (d), triplet (t) and multiple (m). FAB-Mass spectra were recorded on a JEOL SX 102/DA-6000 mass spectrometer/data system using Argon/Xenon (6 kV, 10A) as the FAB gas. The accelerating voltage was 10 kV and the spectra were recorded at room temperature and *m*-nitrobenzyl alcohol was used as the matrix. Molar conductivity measurements were recorded on Remi Conductivity Bridge with a cell having cell constant 0.51 and magnetic moment was carried out using Guoy's balance. Electrochemical behavior of the metal complexes was investigated with CH Instruments, U.S.A (Model CHI 604D) in DMSO containing n-Bu_4NClO_4 as the supporting electrolyte.

Synthesis of ligands (L)

Synthesis of Curcumin derivative-Stage 1 (Knoevenagel Condensation): (1E,6E)-1,7-bis(3,4-dimethoxyphenyl)hepta-1,6-diene-3,5-dione (0.03 mmol) and hydroxyl benzaldehyde were dissolved in methanol (200 mL) and heated to reflux. The reaction mixture was transferred while hot and allowed to cool overnight. The solid that separated was filtered and washed with Et_2O (5 × 50 mL) and dried in a vacuum oven (40^{o}C) to afford dialdehyde as a pale brown solid (75%).

Stage 2: The above product (0.01 mmol) was added with 3-aminonaphthalen-2-ol (0.02 mmol) and reflexed for 6 hrs. The reaction mixture was refluxed at 70–80^{o}C with constant stirring for 3- 5 hrs and the progress of reaction was monitored by TLC. The resulting solid product was isolated and washed with petroleum ether and methanol. The Schiff base was dried in vacuum desiccator over anhydrous $CaCl_2$.The recrystallized ligand was dried in a vacuum dessicator over fused calcium chloride. The synthetic route to the target compounds is outlined in Scheme 1.

Ligand (L): Mol. Formula: $C_{50}H_{42}N_2O_7$, Mol wt. 782. Yield: 65%; CHN analysis: Calcd for; C 76.71, H 5.41, N 3.58; Found: C 76.58, H 5.29, N 3.48. UV (nm): 340, 268 nm. FT-IR (cm^{-1}): 3280 (Ar O–H); 3082-3074 (Ar–H); 2962, 2898 (C–H); 1654 (C=N); 1224 (Ar C–OH). ^{1}H-NMR (ppm): 10.4 (Ar-OH), 6.8-7.9 (Ar-H), 3.6 ppm (Ar-OCH_3).

Synthesis of complexes with ligand

A solution of metal acetate(s) (0.05 M) in 20 mL methanol was added to a stirred solution of ligand (0.05 M) in 20 mL of methanol. The resulting mixture was stirred at room temperature till a precipitate of the complex formed. The precipitate was filtered and washed with cold methanol and hexane. The other metal complexes were prepared using similar procedure. The complexes were dried in a vacuum dessicator over fused calcium chloride.

Copper complex of L: Mol. Formula: $C_{50}H_{40}N_2O_7Cu$. Mol wt.844. Yield: 72%; CHN analysis: Calcd for: C 71.12, H 4.77, N 3.32, Cu 7.53; Found: C 58.22, H 4.14, N 11.08, Cu 12.62. UV (nm): 324, 240 & 546 nm. FT-IR (KBr disc): 3170 (N–H), 1175 (C–N), 1610 (C=N), 540 (M–N), 486 (M–O). FAB mass spectrometry (FAB-MS): *m/z*: 845 [M+1]. μ_{eff}(BM) = 1.88. Λ_m (S cm^2mol^{-1}) =10.

Nickel complex of L: Mol. Formula: $C_{50}H_{40}N_2O_7Ni$. Mol wt. 839. Yield: 60%; CHN analysis: Calcd for; C 71.53, H 4.80, N 3.34, Ni 6.99; Found: C 71.42, H 4.68, N 3.20, Ni 6.82. UV-Vis., (nm): 342, 268, 536 nm. FT-IR (cm^{-1}): 3178 (N–H), 1152 (C–N), 1590 (C=N), 540 (M–N), 482 (M–O). FAB mass spectrometry (FAB-MS): *m/z*: 840 [M+1]. μ_{eff}(BM) = 2.48. Λ_m (S cm^2mol^{-1}) = 16.

Cobalt complex of L: Mol. Formula: $C_{50}H_{40}N_2O_7Co$. Mol wt. 839. Yield: 64%; CHN analysis: Calcd for: C 71.51, H 4.80, N 3.34, Co 7.02. Found: C 71.34, H 4.70, N 3.18, Co 6.90. UV-Vis., (nm): 342, 260, 510 nm. FT-IR (cm^{-1}): 3176 (N–H), 1148 (C–N), 1592 (C=N), 522 (M–N), 470 (M–O). FAB mass spectrometry (FAB-MS): *m/z*: 840 [M+1]. μ_{eff}(BM) = 1.96. Λ_m (S cm^2mol^{-1}) = 20.

Zinc complex of L: Mol. Formula: $C_{50}H_{40}N_2O_7Zn$. Mol wt. 846. Yield: 72%; CHN analysis: Calcd for; C 70.96, H 4.76, N 3.31, Zn 7.73; Found: C 70.60, H 4.54, N 3.22, Zn 7.64. UV-Vis., (nm): 342, 265, 510 nm. FT-IR (cm^{-1}): 3182 (N–H), 1162 (C–N), 1591 (C=N), 542 (M–N), 480 (M–O). FAB mass spectrometry (FAB-MS): *m/z*: 847 [M+1]. μ_{eff}(BM) = 0. Λ_m (S cm^2mol^{-1}) = 15.

DNA binding study

The UV–visible absorption titration method is used to study the DNA binding nature of all the binary metal complexes. The complex concentration was fixed with 10 μM, while varying the CT-DNA concentration from 0-10 μM. Because of the low solubility of complexes in the buffer solution, they were dissolved in DMSO first to get a stock solution, and the stock solution of CT-DNA was prepared by diluting DNA in Tris–HCl/NaCl buffer at pH = 7.2 (50 mM NaCl/5 mM Tris–HCl). A Tris-buffer solution of CT-DNA gave a ratio of 1.8–1.9 of UV absorbance at 260 and 280 nm, indicating that the DNA was sufficiently pure and free of protein [10]. The CT-DNA concentration per nucleotide was measured from its absorbance by employing the molar extinction coefficient value of 6600 M^{-1} cm^{-1} at 260 nm [11]. To measure the absorbance of complex and to eliminate the absorbance of CT-DNA itself, equal quantity of CT-DNA was added to both the complex and the reference solutions and the resulting complex solution was incubated for 4-5 min before absorption spectra were recorded. From the absorption data, the intrinsic binding constant (K_b) was calculated.

Superoxide dismutase activity (SOD)

The superoxide dismutase activity (SOD) of the metal complexes were evaluated using alkaline DMSO as source of superoxide radicals ($O_2^{\bullet-}$) generating system in association with nitro blue tetrazolium chloride (NBT) as a scavenger of superoxide. Add 2.1 ml of 0.2 M potassium phosphate buffer (pH 8.6) and 1 ml of 56 μl of NBT solutions to the different concentration of copper complex solution. The mixtures were kept in ice for 15 min and then 1.5 ml of alkaline DMSO solution was added while stirring. The absorbance was monitored at 540 nm against a sample prepared under similar condition except NaOH was absent in DMSO.

Hydrogen peroxide Assay

A solution of hydrogen peroxide (2.0 mM) was prepared in phosphate buffer (0.2 M, 7.4 pH) and its concentration was determined spectrophotometrically from absorption at 230 nm. The complexes of different concentration and vitamin C (100 μg/ml) were added to 3.4 ml of phosphate buffer together with hydrogen peroxide solution (0.6 mL). An identical reaction mixture without the sample was taken as negative control. The absorbance of hydrogen peroxide at 230 nm was determined after 10 min against the blank (phosphate buffer).

Antimicrobial activities

The *in vitro* antimicrobial activities of the investigated compounds were tested against the bacterial species. Sterile Muller Hinton Agar plates were prepared poured and overnight cultures of bacterial pathogens were swabbed on it. The discs were prepared by using Whatman No: 1 filter paper. The

disc size of about 6mm diameter was made using disc paper puncher. The filter discs were sterilized and stored in its dried form. About 100 µl of metal complexes were poured over the sterile filter paper disc and kept for drying in hot air oven at 45ºC for 2 hours. Muller Hinton Agar plates were prepared and overnight bacterial pathogens broth culture was swabbed on the surface of the agar media. The culture filtrate loaded discs were placed aseptically on the surface of the agar using a disc dispenser or a sterile forceps. The plates were incubated at 37ºC for 24 hours. The inhibitions around the antibiotic discs were measured after incubation.

Central Nervous System (CNS) Depressant Activity Study

Curcumin metal chelates were assessed for effect on the CNS using phenobarbitone-induced sleeping time test in mice [14]. Thirty min after the oral administration of curcumin and its derived complexes (25 mg/kg), vehicle control (1% Tween-80 solution in saline), and intraperitoneal injection of diazepam (1 mg/kg), all mice were injected with phenobarbitone (25 mg/kg, i.p.). The animals were observed for the latent period (time between phenobarbitone administration and loss of righting reflex) and duration of sleep (time between the loss and recovery of righting reflex).

Hypoglycemic Activity Study

The test was performed using a slight modification [15]. The animals were weighed and randomly divided into eight groups consisting of 6 mice in each group. At zero hours fasting blood glucose level from each group was measured from tail vein just prior to glucose administration by using glucometer (Braun G-423 S from Hong Kong) and glucose oxidase-peroxidase reactive strips. To measure the blood glucose level, tail tip of mice was cut with a sharp blade and then little amount of blood was collected and exposed to the touch of glucose test strips. Within seconds blood glucose level was visualized. Nebanol (Bacitracin) ointment was applied on the wound to avoid infection. Then the samples were administered (0.1% saline as control, metformin as standard and curcumin metal chelates) using oral feeding needle. After 1 hour, 2 hours, and 3 hours, blood was collected in the same procedure and blood glucose level was measured to see the hypoglycemic effect of the test sample compared to control and standard groups.

3.5. Statistical Analysis

All the values are expressed as mean ± standard error of the mean (SEM). One-way ANOVA followed by Dunnett's test was used to determine a significant difference between control groups and experimental groups. ≤ 0.001 was considered to be statistically significant.

Ferricyanide reducing assay

Ferric reducing antioxidant power (FRAP) was measured using a modified method of Benzie and Strain [16]. The method is based on the reduction of ferric ions (Fe^{3+}) to ferrous ions (Fe^{2+}). The amount of Fe^{2+} complex can be monitored by measuring the formation of blue color at 700 nm. Increasing absorbance at 700 nm indicates an increase in reductive ability. Different concentrations of the synthetic compounds (0.5–15 µM in DMSO) were mixed with 2.5 ml of phosphate buffer (0.2 M, pH = 6.6) and 2.5 ml of 1% potassium Ferricyanide. Afterwards, the mixture was incubated at 50 °C for 20 minutes. In the next step, at the end of the incubation, 2 ml of 1% trichloroacetic acid was added to the mixture and centrifuged at 3000 rpm for 10 minutes. After centrifugation, the upper 2.5 ml layer was mixed with 2.5 ml of distilled water and 0.5 ml of 0.1% ferric chloride, and the absorbance was measured at 700 nm. The ascorbic acid (1 mg/ml) was used as a standard antioxidant compound.

3. Results and discussion

3.1 Chemistry

The present investigation is focused on analyzing the physicochemical properties of ligand and its metal complexes. The structural characterization, thermal characteristics and surface morphology of

the compounds were studied. The elemental analysis data and the molar conductance behavior of these chelates in DMSO solution suggested the assigned molecular formulae summarized in the experimental section. The structural characterization was accomplished through further spectral investigations, magnetic, thermal (TGA and DTG) and electrochemical measurements. The solid chelates are colored microcrystalline and exhibit shades of green, blue, violet and brown colors. They showed very good solubility in the aqueous medium and the polar organic solvents such as MeOH, DMF and DMSO. They are solids and soluble in DMSO. The formation of product was confirmed by single spot in the TLC. This confirms that the product formation from the condensation reaction followed by cyclization. The prepared compounds and complexes were stable at room temperature (as evidenced from TG measurements). They are in good agreement with theoretical values within the experimental error. All the attempts made to separate suitable single-crystal for X-ray structural analysis were unsuccessful. The electrical molar conductivities values (15- 26 mho mol^{-1} cm^2) at room temperature of 10^{-3} mol L^{-1} in DMF solution of metal complexes with curcumin derivative indicate their nonelectrolytic behavior [17] and confirm the participation of the counter anion in the coordination chromophore or removal of counter ion from complex formation as acetic acid.

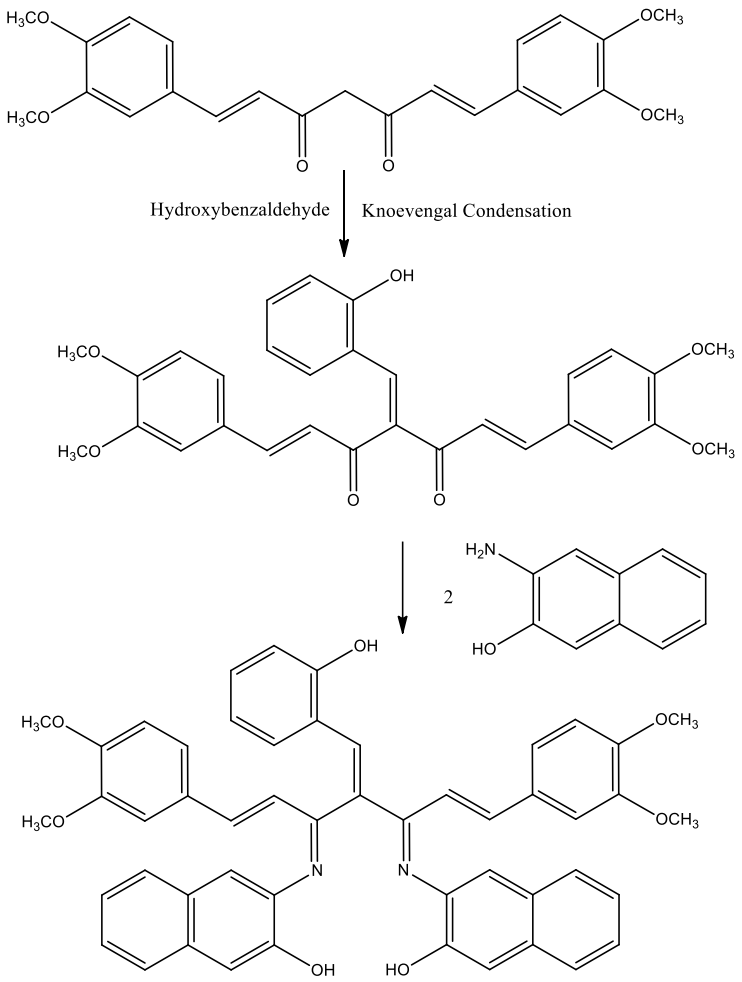

Where
M = Cu(II), Co(II), Ni(II) & Zn(II)

Scheme 1 Schematic representation of synthesis of curcumin derivative

IR study

In the IR spectra of curcumin derivative, the presence of (C=N) and (C-N) stretching frequencies at 1596-1624 and 1244-1258 cm^{-1} in the IR spectrum of the ligand (experimental section) was confirmed the Schiff base formation of Curcumin derivative with 3-aminonaphthalen-2-ol to form

curcumin derivative as ligand (L). The IR spectra of the metal complexes showed a strong band in the region 1662–1640 cm^{-1} which are assignable to the ν(C=N) stretch and shift of this band (20–48 cm^{-1}) to lower frequency indicates the involvement of azomethine nitrogen in coordination. A band at 1359-1374 cm^{-1} was assigned to the vibration frequency of the phenolic C–O group. In the complexes, the band assigned to the vibration frequency of the phenolic C–O group undergoes positive shifts, indicating that the Schiff base is bonded to the metallic ions through the phenolic oxygen atoms. This displacement is to be expected because of the resonance enhancement in the deprotonated ligand upon coordination to the metal center. The IR spectra of all the complexes showed two absorption bands in the far infrared region, 420-440 cm^{-1} and 480-520 cm^{-1}, which are assignable to υ(M-O) and υ(M-N) vibrations, respectively. The FTIR spectral analysis of complexes indicated the presence of all expected functionalities.

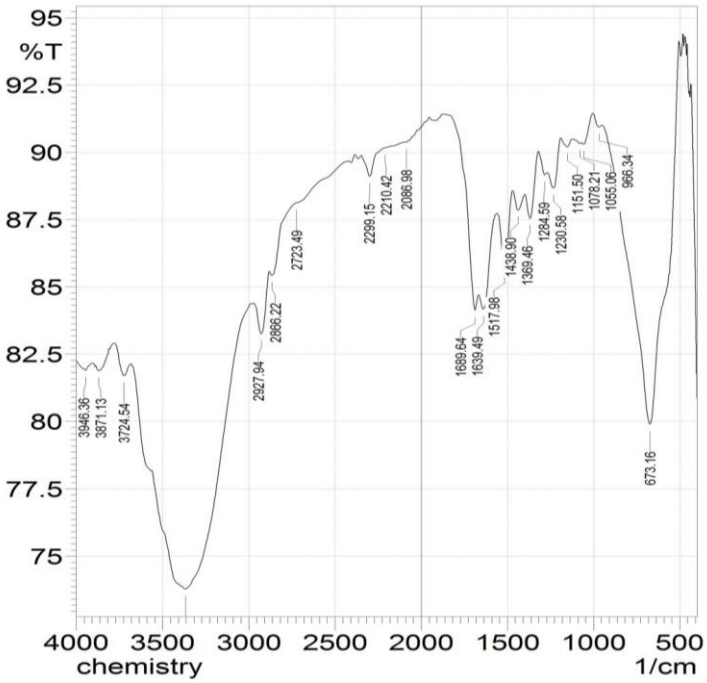

Fig.1 IR spectrum of ligand

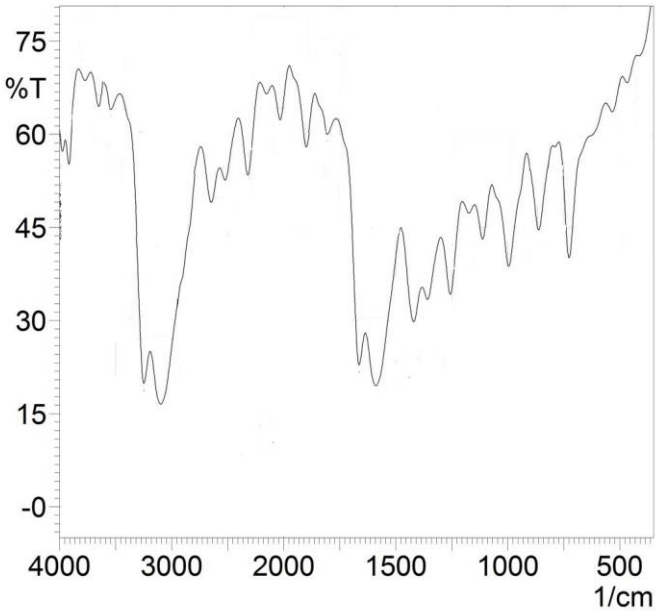

Fig.2 IR spectrum of copper complex

^{1}H NMR study

^{1}H NMR spectrum of the synthesized ligand was measured in $CDCl_3$, with TMS as internal standard. The spectrum data support the formation of the ligand by showing the absence of the characteristic signals due to protons of aldehydic and CH_2 groups. Also, the characteristic singlet peak at 2.20 ppm further confirms the Knoevenagel (HC=C) condensation [17]. Moreover, the spectrum shows also a multiplet at 7.9-6.8 ppm due to the aromatic C-H protons in the aromatic ring protons. In the ^{1}H NMR spectrum of the free ligand, a signal at 10.5 ppm corresponding to the phenolic OH resonance is disappeared in the spectrum of the zinc complex (Fig. 2), which clearly indicates that the Schiff base ligand is coordinated as an anionic ligand to the Zn(II) ion.

FAB mass spectra

Mass spectra provide a preliminary clue for structure elucidation of compounds. These molecular ions of complexes confirmed the stoichiometry of metal complexes as [ML] type. The mass spectral results and elemental analysis are in good agreement with 1:1 (metal:ligand) stoichiometry for the formation of metal complexes. The mass spectrum for ligand and its copper complex are consistent with the proposed formula (molecular ion m/z 783 and 845). In addition, the mass spectra show different peaks representing successive degradation of the complexes with an intensity gives an idea on the stability of the fragments.

Metal-chelating properties of ligand

Several studies suggested that oxidative damage also plays an important role in this chronic neurodegenerative disease. The direct evidences of the oxidative stress hypothesis are increased lipid peroxidation and the increased concentration of Fe, Cu, Al, and Hg in AD patients' brian.11 Thus, therapeutic strategy that aimed at the removal of free radicals or prevention of their formation might be beneficial for AD. Recently, abundant data has implicated the roles of biometals such as iron, copper, and Zinc in the Ab aggregate deposition and neurotoxicity including the formation of reactive oxygen species (ROS). Firstly, abnormal enrichment of Cu, Fe, and Zn in post-mortem AD brain has been confirmed. In vitro experiments revealed that these metals are able to bind to Ab, thus promoting its aggregation. On the other hand, redox-active metal ions like Cu and Fe contribute to the production of ROS and widespread oxidation damages observed in AD brains. Therefore, modulation of such biometals in the brain provides a potential therapeutic strategy for the treatment of AD. Small molecule chelating agents have been proposed for this purpose.

However, poor target specificity and consequential clinical safety of current metal-complexing agents make them undesirable for wide application. To circumvent this drawback, the new strategy of developing bifunctional or multifunctional metal chelators has recently been proposed. In addition to the metal chelating ability, these agents are also designed to improve their uptake across the blood–brain barrier, decrease Ab levels, inhibit cholinesterase and increase anti-oxidant capabilities.

The chelation ability of curcumin derivative with biometals such as Cu, Fe and Zn was studied by UV–vis spectrometry. Electronic spectral of curcumin derivative in ethanol changed in the presence of Cu2+ and Fe2+ ions while remained unchanged after adding Zn2+ ions. Upon the addition of CuSO4 and FeSO4, the curve had a red shift (after adding Cu2+, the peak at 260 nm shift to 285 nm whereas the peak at 420 nm shift to 492 nm) suggesting the formation of curcumin derivative -metal (II).

Thermo gravimetric analysis

Thermal analyses provide valuable information regarding the thermal stability of the complexes in addition to the nature of water/solvent molecules in complexes. It helps us to distinguish the lattice water and coordinated water molecules present in the compound, and also to suggest a general scheme for the thermal decomposition of compounds under study [20]. The thermogram for the

ligand and its complexes was recorded from ambient to 800°C at a heating rate of 10°C/min in a nitrogen atmosphere.

Thermal stability of the metal complexes was investigated under nitrogen atmosphere in the temperature range of 0-800 °C. TGA data of metal complexes have shown two-step decomposition. From the TGA curves, it is observed that there is no decomposition below 200^{o}C for all the metal complexes that confirms all these complexes are free from water molecules in/out of the coordination sphere. In the first step, the complexes showed a sudden weight loss in the temperature range 292-420^{o}C corresponding to departure of partial ligand moiety. In second decomposition step, there is a gradual weight loss appeared in the temperature range of 340-752^{o}C corresponding to the complete thermal decomposition of the organic part around the metal ion, remaining left out was due to metal oxide (MO) and some ashes as the ultimate pyrolysis products.

Electronic absorption spectra

Study the electronic transitions in the ultra violate and visible regions of the metal chelates furnish easy and valuable information about the stereochemistry and the electronic properties of the central metal ion in its coordination environment. In this regard a saturated solutions of the inspected copper(II) were prepared in DMF as suitable solvent and the distinguishing electronic absorption spectra were measured by using the double beam spectrophotometer at the ambient temperature. The electronic spectrum of the free ligand consists of two bands centered at 245 and 262 nm, attributed to the intra ligand π-π* transitions and are red shifted when the ligand is protonated and coordinated to the metal ions (245– 267 nm). In the spectra of metal complexes, these transitions were shifted to lower wave lengths and such changes are the signs the formation of the coordination between metal and ligand due to the donation of the lone pair of electrons by the nitrogen/oxygen of the ligand to the central metal ion. A third band in the electronic spectrum of the ligand at 362 nm, assigned to the n-π* transition which, upon coordination of the ligand, disappears from the electronic spectra of the complexes. The electronic spectrum of the copper complex exhibits bands at 436 nm which can be assigned to $^{2}B_{1g} \rightarrow {}^{2}A_{1g}$ transition. The square-planar geometry of Cu(II) ion in the complex is confirmed by the measured magnetic moments values, 1.88 B.M.

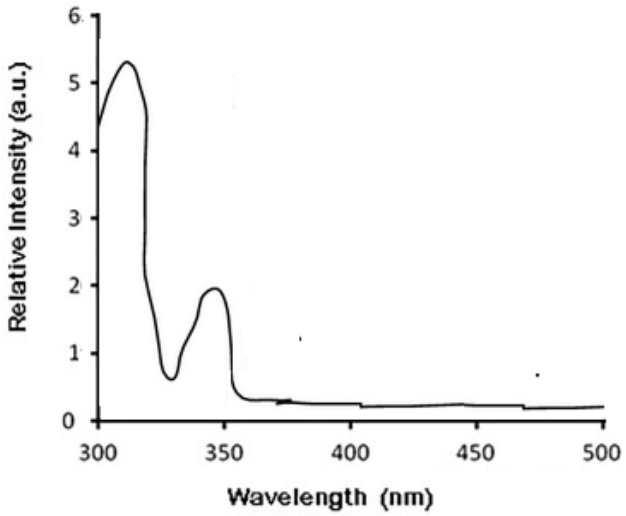

Fig 3. UV Visible spectrum of ligand

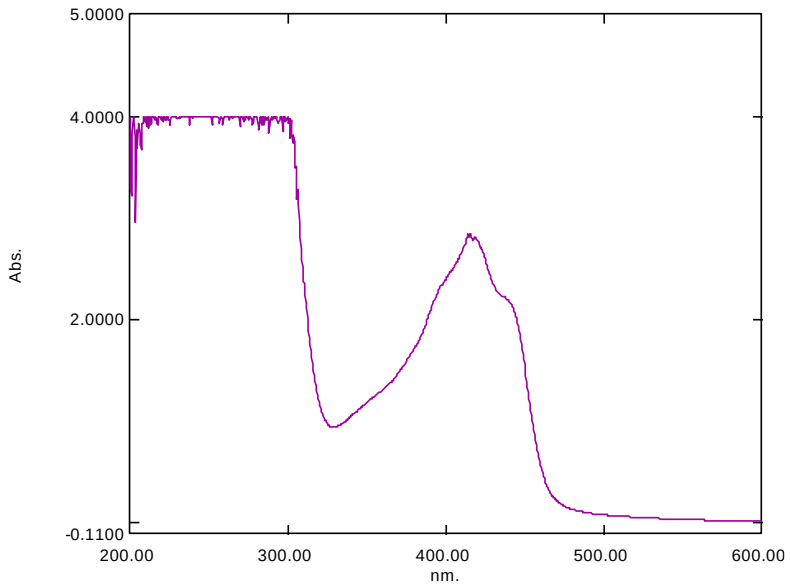

Fig 4. UV Visible spectrum of copper complex

Room temperature magnetic moments in B.M. of the investigated metal(II) chelates were determined to further elucidate the their structural features. The results obtained are presented in the experimental section which demonstrates the magnetic dilute status of all complexes. The observed magnetic moments for all complexes fall in the range 1.94 – 2.15 BM (Table 5) and indicate the monomeric nature of the complexes in a octahedral geometry. This results excluded any metal – metal interaction since the reported μ_{eff} values are slightly higher than the spin only (S=1/2) behavior of 1.73 B.M. for d^9 configuration in a magnetically dilute environment.

ESR spectrum

The clear resolution of the EPR spectra of these copper(II) complexes further confirmed this finding. An investigation was made to see whether the geometry around copper ion is influenced by the presence of a solvent. The 'f' value for Cu, Zn SOD is 160 cm, indicating a tetrahedral distortion from square planar geometry and is one of the features that enhance the catalytic activity of the enzyme. From the above EPR data the f values for copper complexes were determined to be 150-158 (g_{II} / A_{II}). Therefore, the synthesized Cu(II) complexes exhibiting appreciable square planar distortion is expected to show high SOD-like activity and catalytic activity. Based on Kivelson and Neiman hypothesis the trend g|| (2.248– 2.271) > g⊥(2.042 –2.054) is characteristic of the axial symmetry and confirm the presence of the unpaired electron of the d9 configuration is localized in dx2–y2 orbital for copper(II) ion in the square pyramidal stereochemistry [21]. The present ESR together with the position of the d–d absorption bands point out to a square planar and square-pyramidal structures and comparable with analogous copper(II) complexes having the same stereochemistries [22,23]. The tetrahedral distortion which is manifest by the dependence of g|| on the dihedral angle led to the introduction of the quotient g||/A|| as a convenient measure of the degree of that distortion [24]. The EPR data, for the copper complex provide a value of 140 cm, which suggests a slight tetrahedral distortion around the copper atom, in agreement with the solid state X-ray data. Thus, if the conclusion derived from this parameter is consistent with the X-ray data obtained in solid state, we may conclude that the coordination geometry around the metal center is not significantly influenced by the presence of the solvent molecules (DMSO).

DNA interaction studies

The binding of metal complexes with the DNA (along with a myriad of other targets that exist in living cells) is regarded to be one of the possible mechanisms responsible for their cytotoxic potential. In principle, there exist two modes for binding the metal complexes to DNA: covalent and

non-covalent - (which includes electrostatic interactions, groove binding and intercalation between base pairs). An elucidation of the relationship of the DNA - metal complex binding mode *vs* biological activity provides significant information to aid the design of new metal complexes, targeted to DNA, with an improved therapeutic potential.

Electrochemical studies

Our kinetic investigations of the catalytic oxidation of the studied substrates demonstrated the reduction of CuII to CuI by 3,5-DTBC or *o*-APH3 followed by the oxidation of Cu(I) by the atmospheric dioxygen during the catalytic oxidation cycle. In this context, electrochemical behavior of the inspected copper(II) chelates was examined, because the redox potential is an important parameter in electron transfer processes and in our catalytic systems. Methanol was the suitable solvent for performing the cyclic voltammetric measurements versus the reference electrode Ag/Ag+. All complexes exhibit a quasi-reversible peak in the region 310 - 450 mV regenerating from a one-electron reduction of copper(II) to copper(I) followed by the corresponding oxidation of Cu+ to Cu2+. In this situation the couple CuII/CuI is present as a redox centre. Most of the complexes undergo reduction are completely regenerated following electrochemical oxidation, as shown in S25 and S26. The chemically reversibility for one-electron transfer process in the case of CuII/CuI centre is evidenced from the ratio of the peak currents where *i*pa/*i*pc is ≈1.0. The limiting peak-to-peak separation values (_*E*p, 60 - 86 mV), approach the referenced value (_*E*p, is 60 mV) for a reversible one-electron redox process.

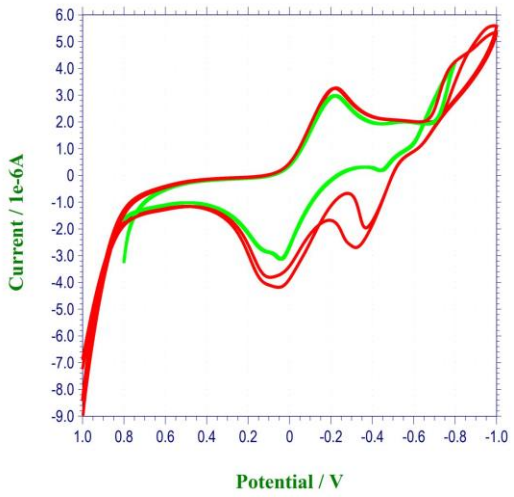

Fig.5. Cyclic votammgram of copper complex in the absence (Red colour) and presence of DNA (Green colour)

Copper (II) complexes containing two functionalities, curcumin and NSAIDs tolfenamic, mefenamic and flufenamic acids, were prepared, with the aim to study their effectiveness as prospective anticancer agents. Specifically, it was aimed to correlate the molecular structure of the complexes with their ability to intercalate into DNA, to interact with albumin, to scavenge superoxide radical anions, and to kill cancer cells. Initially, we now report the structural characteristics of all three complexes both in the solid state and in solution.

SOD-mimetic activity of metal(II) complexes

The SOD mimetic activity of the complexes was determined using an indirect xanthine oxidase (XO) enzyme method in the presence of its natural xanthine substrate (X). The X/XO enzyme system serves as the source of the superoxide radical anion (O2.-), which is scavenged by tetrazolium blue (Nitro-Blue-Tetrazolium (NBT)) and subsequently reduced to a blue-colored formazan. During the course of the reaction, the yellow color of the solution gradually changes to

blue, as a result of NBT reduction. The change in color intensity correlates with the concentration of reduced NBT, i.e. with the amount of superoxide radical anion that has been scavenged. This color change is accompanied by the increase in the intensity of the absorption band at 550-560 nm. When a substance, capable of scavenging superoxide radical is added to the reaction mixture, a competitive reaction takes place, which results in the inhibition of the reaction between NBT and the superoxide radical anion. The slowing of the NBT reduction or its complete termination results in a decrease in its spectral absorbance, which is proportional to the increasing concentration of the added substance (inhibitor). Thus, the rate of the change of absorbance intensity after the addition of the studied complexes was measured, and the *IC*50 values (concentration of the complex causing 50% inhibition of the NBT reduction) were determined from the graphical dependence of the rate of NBT reduction (% inhibition) on the concentrations of the complexes.

It is clear that all three complexes exhibit excellent SOD-mimetic activity, with IC50 values ranging from 0.94 to 1.23 μM (the smaller the value, greater the SOD-mimetic activity). The SOD mimetic activity of complexes decreases in order **Cu-L > Ni-L> Co-L** > **Zn-L**. To assess the effectiveness of SOD mimetic activity, we compared our results with the IC50 values of some anti-inflammatory drug complexes which were determined using the NBT assay under the same conditions. The IC50 values obtained for the complexes indicate that their SOD mimetic activities are within the same range as for other compounds which are known to possess excellent superoxide radical scavenging activities. For comparison, the SOD activity of Cu(II)-indoctain complex, [Cu2(indo)4(H2O)2] is considered an excellent SOD mimetic ,with an IC50 value of 1.31 μM [86]. Indomethacin (indoH) is an acid [1- (4-chlorobenzoyl)-5-methoxy-2-methyl-1H-indole-3-acetic acid] used orally as a highly effective anti-inflammatory drug in veterinary medicine. The studied copper complex showed a greater SOD activity than was determined for the Cu(II)- indomethacin complex.

The mechanisms of the SOD mimetic activity of low-molecular weight Cu(II) complexes can be proposed as follows. First, the superoxide radical anion ($O2^{\cdot-}$) binds to the Cu(II) ion of the complex, followed by electron transfer from the superoxide radical anion to Cu(II) (eqn. 7). The resulting cuprous complex, Cu(I)-L, undergoes redox cycling and is oxidized back to the cupric complex, Cu(II)-L, by a reaction with another molecule of $O2^{\cdot-}$ (eqn. 8) [87]:

The SOD mimetic activity of Cu(II) complexes is affected by a number of factors of which the most critical are: (i) minimal steric barriers to the superoxide radical anion accessing the copper ion and (ii) the rapid exchange of axially coordinated ligands to the copper(II) ion. Considering the fact that the complexes 1-3 exhibit minimal structural differences, it is reasonable to assume that the small differences in SOD mimetic activity may originate in the nature of the distant substituents on the aryl ring (chlorines in complex 1, methyl groups in complex 2 and fluorines in complex 3) and slight differences in the geometry of copper(II) cores of all three metal complexes. To obtain direct experimental evidence for the reduction of Cu(II) complexes by superoxide radical anions, a specific chelator of Cu(I) species, neocuproine was introduced. Cu(I) forms a colored complex with neocuproine (Cu(I)-neocuproine) that absorbs at 458 nm [89]. The redox cycling mechanism was thus confirmed for Cu(II) in all complexes 1, 2 and 3 in the presence of superoxide radical anion (eqns. 7 and 8), and this cycling between cupric and cuprous species (Cu(II) □ Cu(I) □ Cu(II)) explains the formation of superoxide radical anions, hydroxyl radicals and singlet oxygen, all of which contribute to DNA damage.

Antimicrobial activity

Infections caused by microorganisms, like bacteria and fungi, are followed with concerns by the World Health Organization (WHO) due to increasing antimicrobial resistance. Metal based pharmaceuticals are a promising approach to new drugs with different mechanisms of action. The aim of destroying bacterial plasma membranes, which consist of a phospholipid bilayer similar to that of eukaryotic cells, by hydrophobic interactions, brings us again to amphiphilic metal complexes. Our mentioned results are comparable to previously reported biologically active complexes used as drugs. Many compounds possess modified pharmacological potentials when

administered in the form of metal based compounds. Of the metal ions commonly used are cobalt, copper and zinc because of forming low molecular weight complexes and therefore, prove to be more beneficial against several diseases.

The ligand and its metal complexes were tested for their inhibitory effects on the growth of bacteria (Staphylococcus aureus, Escherichia coli, Pseudomonas aeruginosa, Bacillus subtilis). This is attributed to the fact that microorganisms can achieve resistance to antibiotics through biochemical and morphological modifications. The experimental data presented in Table 1 suggested that the metal complexes are more potent in inhibiting the growth of microorganisms than the ligand against the same microorganisms under identical experimental conditions. This may be due to the change in structure due to coordination and chelating trends to make metal complexes act as more powerful and potent bactereostatic agents, thus inhibiting the growth of the microorganisms.

Several factors are known to affect the biological activity of a given molecule. These factors include lipophilicity, chemical structure, resonance, and thermodynamic stability [1,42]. Many dithiocarbazate Schiff bases and their metal complexes have been shown to exhibit a wide range of cytotoxic activities, with small changes in the chemical composition often leading to vast differences in selectivity and activity [42–46]. The complexation of Schiff bases with metal ions reduces the polarity of the metal ions through the partial sharing of positive charge with the donor atoms and p-electron delocalization upon chelation [47]. This results in the enhancement of the lipophilic characteristics of the central metal atom allowing the blocking of cellular enzymatic activity [48].

Moreover, coordination reduces the polarity of the metal ion mainly because of the partial sharing of its positive charge with the donor groups within the chelate ring system formed during the coordination. This would suggest that the chelation could facilitate the ability of a complex to cross a cell membrane and can be explained by Tweedy's chelation theory [41]. The results indicated that the synthesized compounds have better activity towards Gram-positive bacteria than towards Gram negative bacteria. The reason for this may probably be due to the difference of the cell membrane structure, where the outer membrane of Gram-negative bacteria can reduce the damage from the synthesized compounds. This means that the external membrane of Gram-negative bacteria may play a preventive role for the antibacterial effect of the above-mentioned compounds.

The pathogens secreting various enzymes, which are involved in the breakdown of activities, appear to be especially susceptible to inactivation by the ion of complexes. The metal complexes facilitate their diffusion through the lipid layer of spore membrane to the site of action and ultimately killing them by combining with the OH, and C=N groups of certain cell enzymes. The Mn(II), Co(II), Ni(II), Cu(II) and Zn(II) complexes shows greater antibacterial activity towards bacteria. The variation in the activity of the metal complexes against different organisms depends on the impermeability of the microorganism cells or on differences in ribosome of microbial cells [42]. Such a chelation could increase the lipophilic nature of the central metal atoms. chelation dominates, simultaneously other factors such as solubility, dipole moment, stereo chemistry, size, coordination sites, geometry of complexes, concentration and hydrophobicity also influence the antimicrobial potency of the complexes [60-64]. Among all the synthesized metal compounds, the Cu(II) complexes 1a and 2a are more active than Co(II), Ni(II) and Zn(II) complexes.

It can be assumed that the reason for this is that metal complexes can penetrate cells more easily than the ligands alone. Since the donor atoms represent high electron density within the ligand systems, the hydrophobicity of the molecules increases when they are coordinated to metal ions. Adsorption on the lipid-containing cell walls is then supposed to be more easily accomplished. Thus, the permeability of membranes and vital diffusion processes are more strongly disturbed, which results in more facile passage through the cell membrane of bacteria. Such considerations might also apply for fungi, the cell walls of which indeed consist of polysaccharides, but can be decorated with hydrophobic proteins. From logP values, higher hydrophobicity of the metal complexes could be concluded, which renders their adsorption to cell walls more probable. Among the metal complexes, the highest activity was found for the derivatives with the dodecyl chain and

Cu(II) as a metal ion. As in the previous study using the pyrazole-derived cations, high electronegativity (Cu > Co > Ni > Zn) and here, also large atomic radii (Cu > Co > Ni > Zn) are discussed to be favorable for withdrawing electron density from the nitrogen donor atoms and thus, increased hydrophobicity and bactericidal activity of the corresponding metal complexes. The hydrophobic moiety can interact with hydrophobic domains of DNA and proteins, as well as lipids as constituents of cellular membranes, the hydrophilic moiety allows for chemical reactivity towards biomolecules due to inherent Lewis acid or redox properties or, in case of labile metal complexes, tendency for ligand exchange reactions. Additionally, such reactivity can be tuned by the design of the corresponding ligand system.The Cu(II) ion has the smallest radius of the first-row transition metals. This results in the strongest binding of the ligand that plays an important role in ligation and transport upon complexation. In addition, the activity of the Cu(II) complex could be due to other factors such as redox activity, ligand exchange reactions, the existence of metabolic pathways for transport and excretion, and activation of metal-dependent enzymes all of which, could play vital roles in determining the most cytotoxic metal.

Table 1 MIC values of ligand, metal salts and its metal complexes against different microbial species (µg/mL)

Compound/ Standard	*E. coli*	*S. aureus*	*B. subtilis*	*C.albicans*	*A.niger*	*A.flavus*
Ligand, H_2L	92	86	90	98	82	80
[CuL]	30	26	22	20	18	25
[NiL]	46	52	40	36	44	38
[CoL]	40	30	38	35	40	42
[ZnL]	28	35	46	30	38	30
Copper acetate	102	110	108	98	100	112
Nickel acetate	106	110	116	120	132	125
Cobalt acetate	128	144	130	136	140	122
Zinc acetate	116	110	108	114	120	104
Sreptomycin	8	12	6	-	-	-
Nystatin	-	-	-	14	10	15

Antioxidant activity

Ferric reducing antioxidant potential (FRAP)

The antioxidant capacity of 1–4 complexes was examined by using a FRAP assay with vitamin C equivalent as a standard for the comparison of the activity (Fig. 6). The results indicate that all of the four complexes have a ferric reducing antioxidant power, while the highest reducing activity was found for complex 4 containing Cu(II) ion. This may be correlated to the structural geometry and electronic properties of Cu(II) complex which leads to more electron donating ability of HOMO of the Cu(II) complex and hence its act as a reductant. The FRAP values were decreased in the other complexes, but still better than standard vitamin C. Moreover, the reducing power of the complexes increased with increase in concentration.

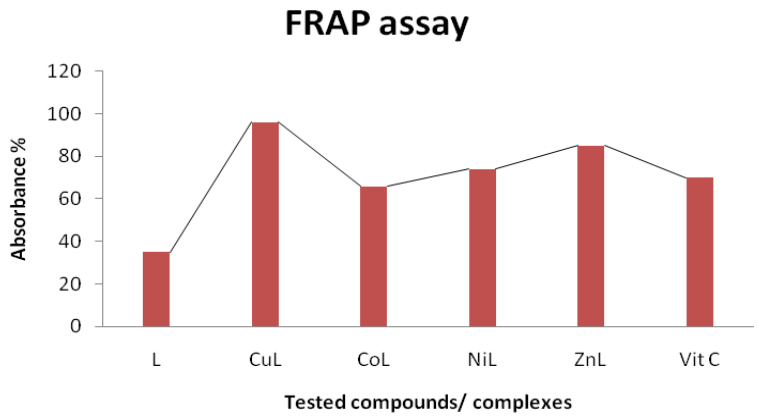

Fig. 6 Ferric reducing antioxidant potential values of ligand, metal(II) complexes and Vitamin C

Peripheral Antinociceptive Activity Study

Curcumin and its metal chelates were subjected to screening for antinociceptive activity by acetic acid-induced writhing inhibition method. Metal complexes effectively reduced the number of abdominal muscle contractions induced by 0.7% acetic acid solution in a dose dependent manner. At the dose of 25 mg/kg body weight, copper, cobalt, and zinc complexes showed significant () antinociceptive activity having 59.15%, 60.56%, and 57.75% of inhibition, respectively, compared to the standard curcumin (54.93%). On the other hand, copper, cobalt, and zinc complexes significantly () demonstrated 73.24%, 74.65%, and 67.60% inhibition of writhing at 50 mg/kg body weight.

Central Antinociceptive Activity Study

In the tail-flick model, reaction time was increased significantly for the test samples and standard drug when compared to the predrug reaction time (control group) 30 minutes after drug administration and thus it appears that the test sample inhibits predominantly the peripheral pain mechanism. Curcumin metal chelates effectively elongated the reaction time in a dose dependent manner. At low doses (25 mg/kg), copper, silver, and zinc complexes showed significant antinociceptive activity after 90 minutes having 102.61%, 101.31%, and 99.02% elongation of reaction time, respectively, compared to the standard morphine (113.40%).

Hypoglycemic Activity Study

The results found from curcumin derivative and its metal complexes showed significant blood glucose lowering activity. The test was performed by taking the samples at the doses 25 mg/kg body weight. Copper, cobalt, and zinc complexes of curcumin showed significant decrease of plasma glucose level. After 3 hours, the plasma glucose levels of copper, cobalt, and zinc complexes of curcumin were 4.72 mmol/L, 4.60 mmol/L, and 4.17 mmol/L, respectively ($P < 0.001$).

Metal complexes significantly ($P < 0.001$) reduced the number of abdominal muscle contractions induced by 0.7% acetic acid solution in a dose dependent manner. At the dose of 25 mg/kg body weight p.o. copper, cobalt, and zinc complexes exhibited higher antinociceptive activity having 59.15%, 60.56%, and 57.75% of writhing inhibition, respectively, than the parent ligand curcumin derivative (54.93%). In tail-flick test, at both doses of 25 and 50 mg/kg, the copper, cobalt, silver, and zinc complexes showed higher antinociceptive activity after 90 minutes than the parent drug curcumin. In elevated plus maze (EPM) model the cobalt and zinc complexes of curcumin derivative showed significant anxiolytic effects in dose dependent manner, while the copper, cobalt, and zinc complexes showed significant CNS depressant and hypoglycemic activity.

Conclusion

The present results concerning the in vitro SA- and DNA-binding of the complexes and their antioxidant activity are promising in regard to the future biological significance of the complexes

towards further studies for their evaluation as potential metallodrugs. Search for drugs of higher efficacy and lower toxicity is a never-ending effort. For the first time, we have reported the in vivo activity of curcumin metal complexes. From these investigations, it may be concluded that curcumin metal chelates showed significant antinociceptive, CNS depressant, and hypoglycemic properties while curcumin and its cobalt and zinc chelates have anxiolytic effects. Among all complexes, the copper, cobalt, and zinc complexes possess higher antinociceptive, anxiolytic, CNS depressant, and hypoglycemic properties than the parent ligand, curcumin. However, studies are required on higher animal model and subsequently on human subjects to prove clinical efficacy of curcumin as an antinociceptive and anxiolytic and further research is essential to find out the possible side effects that it may provide because of central metal of chelation and its principles responsible for such activity.

References

1. Siegel RL, Miller KD, Jemal A (2020) Cancer statistics. CA A Cancer J Clin 70(1):7–30. https://doi.org/10.3322/caac.21590
2. Smith RD, Mallath MK (2019) History of the growing burden of cancer in India: from antiquity to the 21st century. J Glob Oncol 5:1–15. https://doi.org/10.1200/JGO.19.00048
3. Zheng HC (2017) The molecular mechanisms of chemoresistance in cancers. Oncotarget 8(35):59950–59964. https://doi.org/10.18632/oncotarget.19048
4. Schirrmacher V (2019) From chemotherapy to biological therapy: a review of novel concepts to reduce the side effects of systemic cancer treatment (Review). Int J Oncol 54(2):407–419. https://doi.org/10.3892/ijo.2018.4661
5. Wang X, Zhang H, Chen X (2019) Drug resistance and combating drug resistance in cancer. Cancer Drug Resist 2:141–160
6. Salehi B, Machin L, Monzote L, Sharifi-Rad J, Ezzat SM, Salem MA, Merghany RM, El Mahdy NM, Kılıç CS, Sytar O, Sharifi-Rad M, Sharopov F, Martins N, Martorell M, Cho WC (2020) Therapeutic potential of quercetin: new insights and perspectives for human health. ACS Omega 5(20):11849–11872. https://doi.org/10.1021/acsomega.0c01818
7. Lesjak M, Beara I, Simin N, Pintać D, Majkić T, Bekvalac K, Orčić D, Mimica-Dukić N (2018) Antioxidant and anti-inflammatory activities of quercetin and its derivatives. J Funct Foods 40:68–75. https://doi.org/10.1016/j.jff.2017.10.047
8. Xu D, Hu M-J, Wang Y-Q, Cui Y-L (2019) Antioxidant activities of quercetin and its complexes for medicinal application. Molecules 24(6):1123–1138. https://doi.org/10.3390/molecules24061123
9. Torreggiani A, Tamba M, Trinchero A, Bonora S (2005) Copper (II)–quercetin complexes in aqueous solutions: spectroscopic and kinetic properties. J Mol Struct 744–747:759–766
10. De Castilho TS, Matias TB, Nicolini KP, Nicolini J (2018) Study of interaction between metal ions and quercetin. Food Sci Human Wellness 7(3):215–219. https://doi.org/10.1016/j.fshw.2018.08.001
11. Liu Y, Guo M (2015) Studies on transition metal-quercetin complexes using electrospray ionization tandem mass spectrometry. Molecules 20(5):8583–8594. https://doi.org/10.3390/molecules20058583
12. Ahmadi SM, Dehghan G, Hosseinpourfeizi MA, Dolatabadi JE, Kashanian S (2011) Preparation, characterization, and DNA binding studies of water-soluble quercetin--molybdenum(VI) complex. DNA Cell Biol 30(7):517–523. https://doi.org/10.1089/dna.2010.1205
13. Khater M, Ravishankar D, Greco F, Osborn HMI (2019) Metal complexes of flavonoids: their synthesis, characterization and enhanced antioxidant and anticancer activities. Future Med Chem 11(21):2845–2867. https://doi.org/10.4155/fmc-2019-0237

14. Da Silva WMB, de Oliveira PS, Alves DR, de Morais MS (2020) Synthesis of quercetin-metal complexes, in vitro and in silico anticholinesterase and antioxidant evaluation, and in vivo toxicological and anxiolitic activities. Neurotox Res 37(4):893–903. https://doi.org/10.1007/s12640-019-00142-7
15. Ulusoy HG, Sanlier N (2020) A minireview of quercetin: from its metabolism to possible mechanisms of its biological activities. Crit Rev Food Sci Nutr 60(19):3290–3303. https://doi.org/10.1080/10408398.2019.1683810
16. Massi A, Bortolini O, Ragno D, Bernardi T, Sacchetti G, Tacchini M, De Risi C (2017) Research progress in the modification of quercetin leading to anticancer agents. Molecules 22(8):1270. https://doi.org/10.3390/molecules22081270
17. Chen X, Wu X, He Z, Zhang J, Cao Y, Mao D, Feng C, Tian B, Chen G (2020) Molecular docking-assisted design and synthesis of an anti-tumor quercetin-Se(IV) complex. New J Chem 44(20):8434–8441. https://doi.org/10.1039/C9NJ06136C
18. Roy S, Banerjee S, Chakraborty T (2018) Vanadium quercetin complex attenuates mammary cancer by regulating the P53, Akt/mTOR pathway and downregulates cellular proliferation correlated with increased apoptotic events. Biometals 31(4):647–671. https://doi.org/10.1007/s10534-018-0117-3
19. Li S, Zhao Q, Wang B, Yuan S, Wang X, Li K (2018) Quercetin reversed MDR in breast cancer cells through down-regulating P-gp expression and eliminating cancer stem cells mediated by YB-1 nuclear translocation. Phytother Res 32(8):1530–1536. https://doi.org/10.1002/ptr.6081
20. Zhou Y, Zhang J, Wang K, Han W, Wang X, Gao M, Wang Z, Sun Y, Yan H, Zhang H, Xu X, Yang D-H (2020) Quercetin overcomes colon cancer cells resistance to chemotherapy by inhibiting solute carrier family 1, member 5 transporter. Eur J Pharmacol 881:173185. https://doi.org/10.1016/j.ejphar.2020.173185
21. Shin SC, Choi JS, Li X (2006) Enhanced bioavailability of tamoxifen after oral administration of tamoxifen with quercetin in rats. Int J Pharm 313(1-2):144–149. https://doi.org/10.1016/j.ijpharm.2006.01.028
22. Mohana S, Ganesan M, Agilan B, Karthikeyan R, Srithar G, Mary RB, Ananthakrishnan D, Velumurugan D, Rajendraprasad N, Ambudkar SV (2016) Screening dietary flavonoids for the reversal of P-glycoprotein mediated multidrug resistance in cancer. Mol BioSyst 12(8):2458–2470. https://doi.org/10.1039/C6MB00187D
23. Kim MK, Choo H, Chong Y (2014) Water-soluble and cleavable quercetin-amino acid conjugates as safe modulators of P-glycoprotein based multidrug resistance. J Med Chem 57(17):7216–7233. https://doi.org/10.1021/jm500290c
24. Nolan JP, Hare MDDK, McDevitt MDJJ, Ali MVMD (1977) In vitro studies of intestinal endotoxin absorption I. Kinetics of absorption in the isolated everted gut sac. Gastroenterology 72(3):434–439
25. Alam MA, Al-Jenoobi FI, Al-mohizea AM (2011) Everted gut sac model as a tool in pharmaceutical research: limitations and applications. J Pharm Pharmacol 64:326–336
26. Mondal P, Bose A (2019) Spectroscopic overview of quercetin and its Cu (II) complex interaction with serum albumins. Bioimpacts 9(2):115–121. https://doi.org/10.15171/bi.2019.15
27. Kalinowska M, Świderski G, Matejczyk M, Lewandowski W (2016) Spectroscopic, thermogravimetric and biological studies of Na(I), Ni(II) and Zn(II) complexes of quercetin. J Therm Anal Calorim 126(1):141–148. https://doi.org/10.1007/s10973-016-5362-5
28. Dehghan G, Khoshkam Z (2012) Tin (II)-quercetin complex: synthesis, spectral characterization and antioxidant activity. Food Chem 131(2):422–426. https://doi.org/10.1016/j.foodchem.2011.08.074
29. Wilson TH, Wiseman G (1954) The use of sacs of everted small intestine for the study of the transference of substances from the mucosal to the serosal surface. J Physiol 123:116–125.

30. Challa VR, Ravindra Babu P, Challa SR, Johnson B, Maheswari C (2013) Pharmacokinetic interaction study between quercetin and valsartan in rats and in vitro models. Drug Dev Ind Pharm 39(6):865–872. https://doi.org/10.3109/03639045.2012.693502
31. Adukondalu D, Shravan Kumar Y, Vamshi Vishnu Y, Shiva Kumar R, Madhusudan Rao Y (2010) Effect of pomegranate juice pre-treatment on the transport of carbamazepine across rat intestine. DARU J Pharm Sci 18:254–259
32. Bedada SK, Appani R, Boga PK (2017) Capsaicin pretreatment enhanced the bioavailability of fexofenadine in rats by P-glycoprotein modulation: in vitro, in situ and in vivo evaluation. Drug Dev Ind Pharm 43(6):932–938. https://doi.org/10.1080/03639045.2017.1285310
33. Yumoto R, Murakami T, Nakamoto Y, Hasegawa R, Nagai J, Takano M (1999) Transport of rhodamine 123, a P-glycoprotein substrate, across rat intestine and Caco-2 cell monolayers in the presence of cytochrome P-450 3A-related compounds. J Pharmacol Exper Ther 289:149–155
34. Li M, Si L, Pan H, Rabba AK, Yan F, Qiu J, Li G (2011) Excipients enhance intestinal absorption of ganciclovir by P-gp inhibition: assessed in vitro by everted gut sac and in situ by improved intestinal perfusion. Int J Pharm 403(1-2):37–45. https://doi.org/10.1016/j.ijpharm.2010.10.017
35. Sultana N, Arayne MS, Naveed S (2010) Simultaneous determination of captopril and statins in API, pharmaceutical formulations and in human serum by RP-HPLC. J Chin Chem Soc 57(3A):378–383. https://doi.org/10.1002/jccs.201000056
36. Ruan LP, Chen S, Yu BY, Zhu DN, Cordell GA, Qiu SX (2006) Prediction of human absorption of natural compounds by the non-everted rat intestinal sac model. Eur J Med Chem 41(5):605–610. https://doi.org/10.1016/j.ejmech.2006.01.013